Sun, Xin; Shiono, Koji

Modelling of Velocity and Boundary Shear Stress for One-Line Vegetation along the Edge of Floodplain in Compound Channel

MODELLING OF VELOCITY AND BOUNDARY SHEAR STRESS FOR ONE-LINE VEGETATION ALONG THE EDGE OF FLOODPLAIN IN COMPOUND CHANNEL

Xin Sun[1] and Koji Shiono[2]

[1] Researcher, Department of Civil and Building Engineering, Loughborough University, Leicestershire, LE11 3TU, UK; e-mail: X.Sun4@lboro.ac.uk
[2] Professor, Department of Civil and Building Engineering, Loughborough University, Leicestershire, LE11 3TU, UK; e-mail: K.Shiono@lboro.ac.uk

ABSTRACT

Emergent vegetation such as trees, shrubs and bushes, commonly occurs along the banks of river and edges of floodplain, both naturally and by design for erosion prevention and habitat creation, but little is known of the effect of such marginal vegetation on hydraulic processes during flood. In order to understand such effect, experiments were conducted in a compound channel with one-line vegetation to measure boundary shear stress with a Preston tube and velocity with a pitot tube. The boundary shear stress distributions in the main channel and floodplain were significantly different from those of a typical compound channel flow case. With those data, the drag force caused by rods, as vegetation, at the interface was worked out through apparent shear stress analysis and then the drag force is related to roughness height, ks, in order to predict depth averaged velocity and boundary shear stress using Shiono and Knight Method (SKM).

Keywords: compound channel, vegetation, drag force, roughness height, SKM

1. INTRODUCTION

In the last two decades, numerous measurements of flow in straight compound channels with and without vegetated floodplain have been undertaken in small and large-scale physical models in order to improve our understanding of flow mechanisms, (Sellin 1964; Knight & Lai 1985; Shono & Knight 1991; Tominaga & Nezu, 1991). This has led to a better understanding of overbank flow behaviour and to the development of numerous quasi two-dimensional models to predict the lateral distributions of both depth-averaged velocity and bed shear stress. One of which is the Shiono & Knight method (SKM), (1991) that is currently in use by practitioners, as a modelling philosophy, for a 'Conveyance Generator' (CG) with the Roughness Advisor (RA) in Conveyance Estimation System (CES) developed by HR Wallingford, in the UK. At the present, this model does not deal with emergent and submerged vegetation or one-line vegetation for predicting boundary shear stress since the Roughness Advisor uses a Manning coefficient concept including both bed friction and drag force together.

Vegetation is good for river bank protection, ecological equilibrium and landscape, therefore vegetation along a compound channel is increasingly interesting to engineers to consider its impact on environment and water level during floods. River vegetation has been traditionally considered to produce high flow resistance and consequently to decrease the channel conveyance capacity or to increase water level (Petryk & Bosmajian 1975; Kouwen & Fathi-Moghadam 2000). Most of the experimental and numerical investigations of the vegetated channel flow have been carried out in partly-vegetated open channels (Tsujimoto

1992; Nepf & Vivoni 2000; Nezu & Onitsuka 2001) and compound channels with uniformly vegetated floodplain (Pasche & Rouve 1985; Rameshwaran & Shiono 2007).

One-line trees are often planted along the edge of the floodplain for landscape in the river basin (Figure 1) and have three main advantages: efficiency of conveyance of flood water due to less drag force caused by the vegetation, an increase in capacity of flood water storage, and less vegetation maintenance work when compared to the compound channel with trees planted in the whole floodplain. Flow characteristics of compound channels with the whole vegetated floodplain have been studied, but the flow characteristics of the compound channel with one-line trees along the edge of the floodplain have not been reported to date.

Figure 1 River Severn UK.

Figure 2 Experimental compound channel.

To better utilize one-line trees for environmental flood management, there are many uncertainties in its effect on drag force, fluid mixing and sediment transport. This paper therefore investigates the effect of trees along the edge of the floodplain on flow structure, boundary shear stress distribution and drag force based on the experiment. The experiment is conducted in compound channel with one-line rods at the edge of the floodplain as shown in Figure 2, and some suggestions for engineering application (SKM) are made.

2. METHODOLOGY

Measurements were conducted in a 12 m long and 0.306 m wide Perspex tilting flume in the hydraulic laboratory at Loughborough University. Figure 3 illustrates the cross-section shape of the compound channel and the geometrical parameters are B_m = 0.12 m, B_f = 0.15 m, B_s = 0.036 m and s = 1. The flume bed slope (S_0) was set to be 0.001. The flume re-circulates water in a 3 m long and 1.3 m wide steel outlet tank through a circular PVC pipe with a centrifugal pump. The flow rate (Q_d) under uniform flow condition was measured by weighing the outlet water mass per unit time. To minimize the effect of inlet turbulence on the flow development, a 0.1 m long Kraft honeycomb with uniform hexagonal holes was placed at the inlet to straighten the flow and a 0. 25 m long float foam plate was fixed to the honeycomb to avoid the wavy water surface propagating downstream. The uniform flow was obtained by adjusting the weir height at the flume outlet. The water depth was measured by a digital point gauge.

Circular wood rods were used to model emergent vegetation. The diameter (D) and height (H_v) of all rods were 9 mm and 10 cm respectively. A special frame, as shown in Figure 2, was designed to hold one-line rods at y = 0.163 m along the floodplain edge. Based on the suggested critical spacing ratio of $l/D = 3.8$ (Igarashi 1984), a rod spacing value of 0.04 m (l/D=4.4) was used in the experiments. Detailed experimental conditions of no rod and rod cases are listed in Table 1.

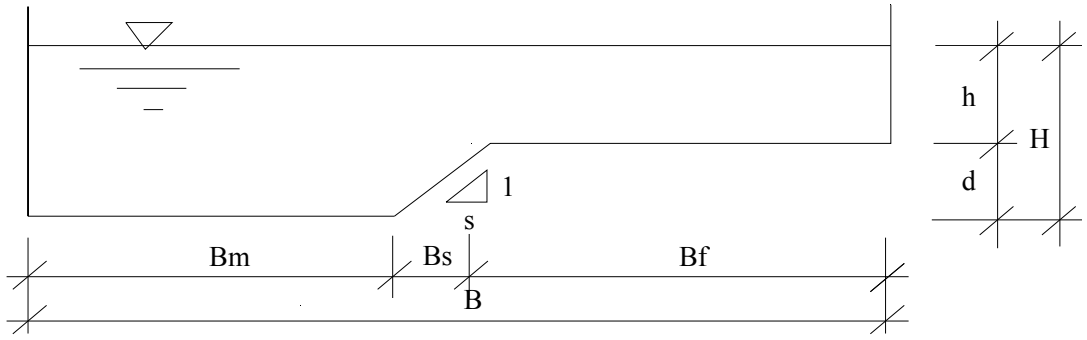

Figure 3 Cross section of compound open channel.

Table 1 Experimental conditions for no-rod and rod cases

Case	Discharge Q (m^3/s)	Main Channel Water Depth H (m)	Relative Water Depth Dr	Reynolds Number Re	Rod Spacing l (m)
S1	0.002200	0.0475	0.24	23163	No rods
S2	0.003521	0.0575	0.37	35218	
S3	0.005430	0.0723	0.50	50569	
R1	0.001739	0.0475	0.24	18310	0.04
R2	0.002422	0.0575	0.37	24225	0.04
R3	0.003500	0.0745	0.52	32265	0.04

The velocity and boundary shear stress were measured with a pitot tube and a Preston tube. Both pitot tube and Preston tube techniques require pressure difference (Δp) between static and dynamic pressures to estimate velocity and boundary shear stress. The pressure difference was obtained from a LPM5480 low-range pressure transducer. The voltage (V_p) and the pressure difference (Δp) were calibrated by changing the water level from 10mm to 50mm in a calibration tank using a digital calliper. Their relationship was worked out and expressed in the form of $\Delta p = 68.913V_p - 3.5209$. The diameter of the inner tube of the Pitot tube is 2.2 mm. The Pitot tube was placed against the flow direction to measure the pressure difference between the static and dynamic pressures. A point gauge and a horizontal ruler were used to control the position of the pitot tube. To ensure the measurement quality, reference readings before and after every experiments were recorded and checked. The record time was set as one minute.

As for a Preston tube, the diameters of the static and dynamic pressure pipes are 3.00mm and 2.72mm, respectively. The record time was set as three minutes. Patel's method (Patel 1965) was adopted to determine the boundary shear stress (τ_b) in this work.

Measurement section was at 8.5 m downstream from the flume inlet, where the flow was fully developed (Sun 2007). Measurement grids in the main channel were 1.5 cm interval in the lateral direction and H/7 interval in the vertical direction, and those in the floodplain varied with case by case. For the rod case, measurements were performed at two cross-sections, namely at the rod and at the centre between two rods. The measured discharge (Qp) from the pitot tube was worked out by integrating the velocities across the cross-section. The error between Qp and Qd was within ±5% for all experiments. The measured averaged cross-section boundary shear stress (τ_{Bp}) was worked out by integrating τ_b across the cross-section. The error between τ_{Bp} and the theoretical overall boundary shear

stress ($\tau_0 = \rho g R S_0$) was within ±5% for no rod case, where ρ and R are the water density and the hydraulic radius respectively.

3. MEAN FLOW PARAMETERS

Figures 4a and 4b show the normalized velocity (U/U_m) pattern at a relative water depth (Dr) of 0.50 in no rod and rod cases. U_m is the section mean velocity. For no rod case S3, in Figure 4a there is a typical velocity bulge of compound channel near the junction of the main channel and the floodplain (MC-FP junction). This bulging pattern is similar to those of Shiono and Knight (1989) and Tominaga & Nezu (1991). They have explained that this cause is owing to the secondary currents and transferring momentum fluid from the main channel to the floodplain.

For rod case R3, see Figure 4b, at the same relative water depth, there is a significant change of isovels due to the effect of rods when compared to no rod case. As can be seen from the figure, there is a high velocity zone in the main channel and on the floodplain, where occurs differently from no rod case. The maximum velocity zone moves further towards the main channel wall in the main channel and towards floodplain wall on the floodplain. This is caused by unbalance of shear force between the walls and the MC-FP junction and as well as by secondary flow inducing the velocity dip phenomenon described by Nezu & Nakagawa (1993).

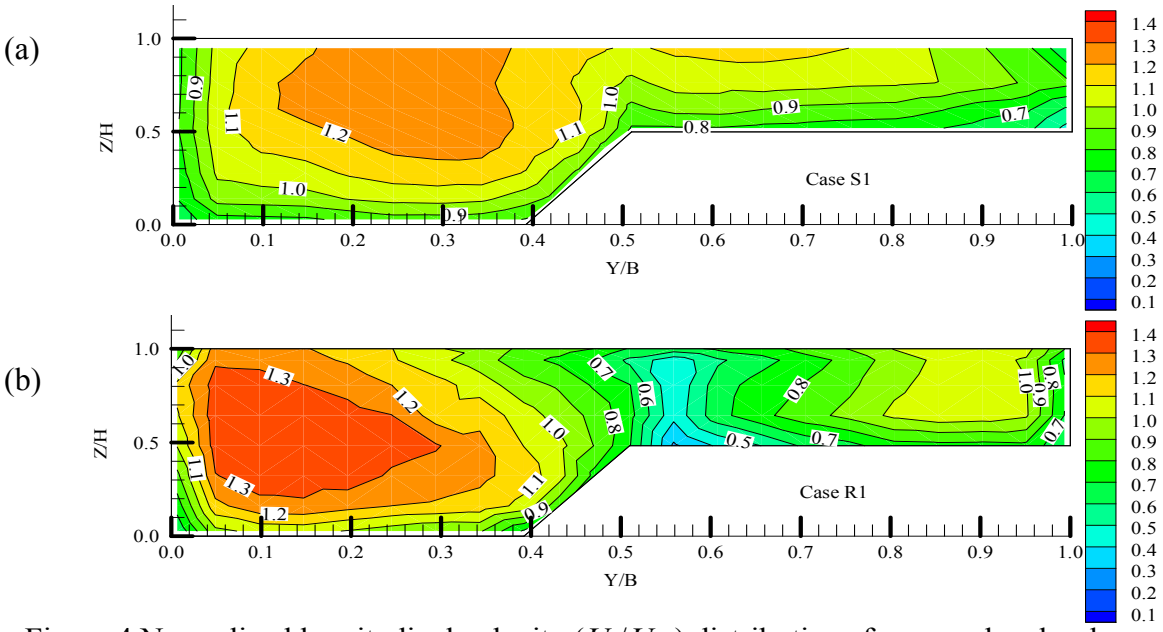

Figure 4 Normalized longitudinal velocity (U/U_m) distributions for no-rod and rod cases. (a) no rod case S3; (b) rod case R3.

There is also a steeper lateral gradient of velocity either side of the MC-FP junction in rod case than in no rod case, indicating that there is a strong shear layer in the main channel and on the floodplain of compound channel for one-line emergent rod case.

4. BOUNDARY SHEAR STRESS

The difference between the measured boundary shear stress, τ_b, and ρgHS_0 for a two-dimensional flow case, was worked out and normalized by ρgHS_0 and is shown in Figure 5 for no rod and rod cases. It is noted that the integration of the difference with respect to the lateral direction gives apparent shear force distribution. For no rod case, the difference shows 0.3 ~0.5 in the main channel, meaning that the boundary shear stress is 30%~50% smaller than ρgHS_0, and the difference does not change as water depth increases. On the side slope, there is the transition of the difference from a positive value to a negative value, meaning that the boundary shear stress is changing from smaller than ρgHS_0 to larger. The peak occurs around the edge of the floodplain. The magnitude starts decreasing from the floodplain edge towards the floodplain wall and becomes zero, and the sign of the difference finally becomes positive near the wall. This variation is associated with momentum transfer from main channel to floodplain and as well as secondary currents explained by Shiono & Knight (1991).

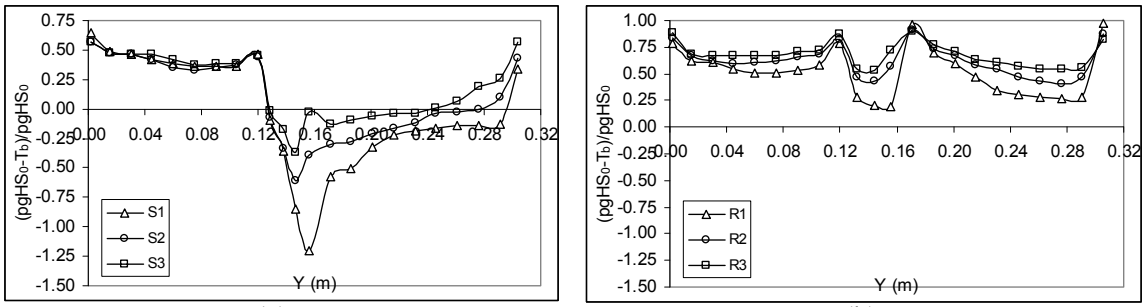

Figure 5 Normalized $(\rho gHS_0 - \tau_b)/\rho gHS_0$ distributions for no-rod and rod cases.
(a) no-rod cases S1 ~ S3; (b) rod cases R1 ~ R3.

As for rod case, the difference is always positive across the compound channel and is above 0.5 in the main channel and larger than no rod case. The pattern of the difference in the main channel is similar to that of no rod case. Apart from the near rod area and floodplain wall, the difference on the floodplain decreases towards the floodplain wall, but never becomes negative, like no rod case. This suggests that there is much less momentum transfer from the main channel to floodplain, like a typical compound flow characteristic. The magnitude varies considerably with water depth. It is noticeable that the difference becomes smaller around the edge of floodplain where the rods are placed. This means that τ_b is increasing as the flow approaches near the rod. This is expected from the flow contraction near the rod, becoming flow faster (velocity squared is proportional to τ_b). From the above there is much less momentum transfer from the main channel to the floodplain like no rod case. Therefore the drag force due to rods is much larger than a typical momentum transfer of compound channel, and thus acts as flow resistance to reduce boundary shear stress both in the main channel and floodplain.

5. DRAG FORCE

The force balance method was used to calculate the total drag force in vegetated compound channel. Under uniform flow condition, the sum of the total boundary shear force and the total drag force is equal to the weight component of flow in vegetated compound channel, which is expressed in Equation 1:

$$\int_P \tau_b (1+s^{-2})^{0.5}\, dp + F_D = \rho g A S_0 \qquad (1)$$

where P is the wetted parameter, A is the channel cross-section area.

From this equation, the total drag force (F_D) per unit channel length was calculated using the measured boundary shear stress along the wetted perimeter. Figure 6 shows the absolute values of the total boundary shear force, total drag force and the weight component per unit channel length for rod cases. The drag force component is higher than the boundary shear force component for higher relative water depth conditions. Figure 7 shows the linear relationship between the total drag force (F_D) per unit channel length and the relative water depth (Dr) for rod cases.

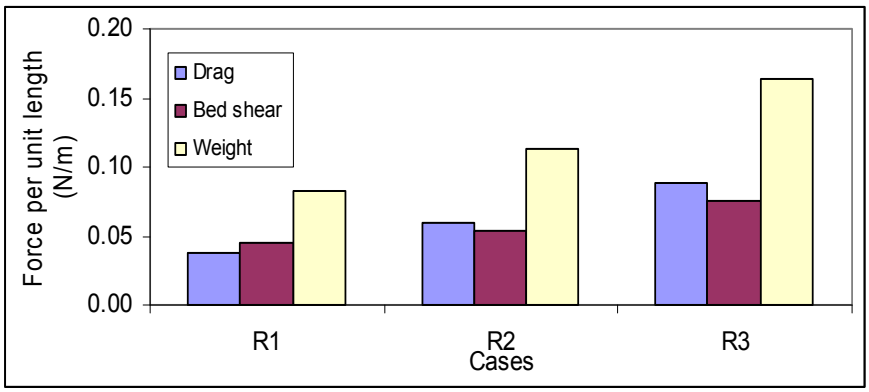

Figure 6 Bed shear force, drag force and weight components per unit channel length.

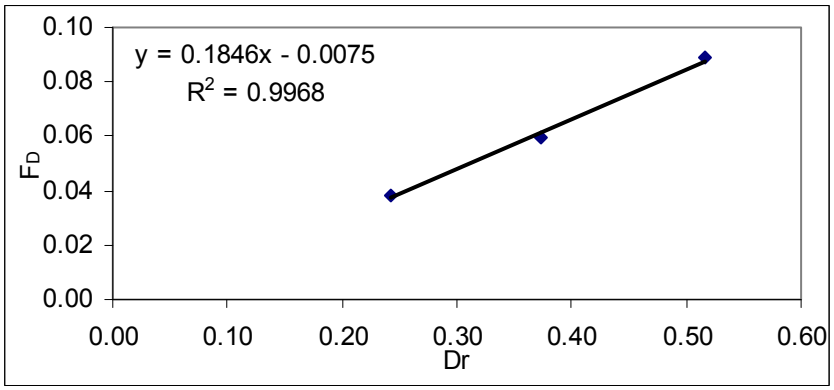

Figure 7 Relationship between the total drag force and the relative water depth.

6. SHIONO AND KNIGHT METHOD (SKM)

Shiono and Knight (1991) proposed the depth averaged momentum equation in the longitudinal direction for uniform flow in the compound open channel, as given by Equation 2:

$$\alpha \frac{\partial}{\partial y}\left[H(y)\left(\rho \overline{UV}\right)_d\right] = \alpha \rho g S_0 H(y) - \alpha \tau_b \sqrt{1+s^{-2}} + \alpha \frac{\partial\left(H(y)\overline{\tau_{yx}}\right)}{\partial y} - S_x H(y) \qquad (2)$$

where, α is the porosity, x, y, z are the longitudinal, lateral and vertical directions respectively; $\overline{U},\overline{V},\overline{W}$ are the temporal mean velocity components in the x, y, z directions respectively; ρ is the density of water; g is the gravitational acceleration; S_0 is the bed slope of the channel and S_x is the source term; τ_b is the bed shear stress; $H(y)$ is the local water depth; s is the bank slope (1:s), $\left(\rho\overline{U}\overline{V}\right)_d = \frac{1}{H(y)}\int_0^{H(y)} \rho\overline{U}\overline{V}dz$, and $\bar{\tau}_{yx} = \frac{1}{H(y)}\int_0^{H(y)}\left(-\rho\overline{uv}\right)dz$.

The bed shear stress τ_b and the depth-averaged Reynolds shear stress $\left(\overline{\tau_{yx}}\right)$ can be determined from Equation 3:

$$\tau_b = \frac{f}{8}\rho U_d^2, \quad \overline{\tau_{yx}} = \rho\bar{\varepsilon}_t\frac{\partial U_d}{\partial y} \quad \text{and} \quad \bar{\varepsilon}_t = \overline{\lambda_{tb}}\left(\frac{f}{8}\right)^{\frac{1}{2}}U_* H(y) \tag{3}$$

where f is the local friction factor, U_d is the depth-averaged longitudinal velocity and $\bar{\varepsilon}_t$ is the depth-averaged eddy viscosity. where $\overline{\lambda_{tb}}$ is the depth-averaged dimensionless eddy viscosity. $H(y)$ is the local water depth and U_* is the friction velocity.

For no vegetation case, the source term S_x is zero. For the emergent vegetation case, the source term S_x is drag force per unit water volume and modelled with $S_x = \sum F_{ei} = \sum \frac{1}{2}\rho\left(C_D S_F A_P\right)_i U_d^2$, where F_{ei} is the drag force of i vegetation per unit fluid volume, C_D is the drag coefficient, S_F is the shading factor, A_P is the projected area of i vegetation per unit fluid volume.

For emergent one-line rod case in this study, $S_x H(y)$ can be given by:

$$S_x H(y) = \frac{N\frac{1}{2}\rho C_D S_F DhU_d^2}{DLh}h = \frac{N\frac{1}{2}\rho C_D S_F DhU_d^2}{DL} = \tau_{br} = \frac{1}{8}\rho f_r U_d^2 \tag{4}$$

where L is the channel length, N is the rod number, τ_{br} and f_r are the drag stress and friction factor caused by the emergent rods, respectively.

Model input parameters

In order to solve Equation 2 for the depth-averaged velocity U_d, the channel geometry, boundary conditions, porosity α, local friction factor f and equivalent friction factor f_r, eddy viscosity and advection term Γ are required as input data.

In the past, velocity was set to zero at walls for the boundary conditions; however, this does not give an accurate velocity near the wall, especially in narrow channels. Imposing mean wall velocities as boundary conditions, the depth-averaged velocity and boundary shear stress can be well predicted in narrow compound channel flow cases (Sun 2007). The mean wall velocities from the experimental data (U_{wall}) were imposed as the boundary conditions to consider the strong wall effects in this case.

Porosity (α) was introduced in the model equation to consider the blockage effect of emergent rods and was calculated with $\alpha = 1 - \frac{V_{rod}}{V_w}$, where V_{rod} and V_w are total volumes of rods and water in the channel respectively.

The modified Colebrook – White equation of Rameshwaran and Shiono (2007) as given by Equation 5 was used to calculate the local friction factor f for a smooth bed.

$$f = \left[-2\log\left(\frac{3.02\upsilon}{\sqrt{128gH^3 S_0}} + \frac{k_s}{12.30H} \right) \right]^{-2} \tag{5}$$

where υ is the kinematic viscosity of water.

The roughness height k_s is used to determine the friction factor f across the channel. Based on the local friction factors outside the shear layer calculated from experimental data of U_d and τ_b, k_s was found to be 0.0003m. To determine the equivalent roughness height k_{sr} due to the drag force, the total drag force (F_D) as shown in Figure 7 was used to determine the equivalent bed shear stress (τ_{br}) using equation (4) and then the roughness k_{sr} value was worked out by equation (5). Table 2 shows the equivalent roughness height k_{sr} for rod case.

Table 2 Roughness heights for rod cases (m)

Cases	R1	R2	R3
Rod Area (k_{rs})	0.0841	0.1644	0.2921
Bed (k_s)	0.0003	0.0003	0.0003

The dimensionless eddy viscosity ($\overline{\lambda_{tb}}$) in the depth-averaged eddy viscosity ; $\overline{\varepsilon_t}$ was set to a standard value of 0.067.

The advection term, (Beta=$\Gamma/\alpha\rho gHS_0 = \partial\left[H\left(\rho\overline{UV}\right)_d\right]/\partial y/\alpha\rho gHS_0$), was worked out using above equations and experimental data.

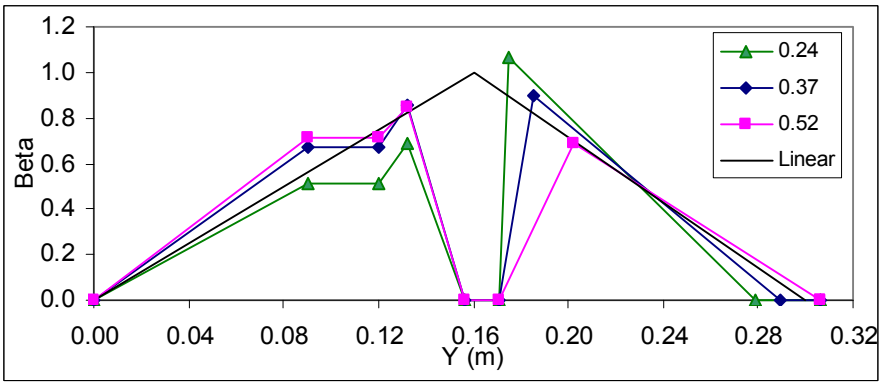

Figure 8 Γ across the channel section for rod case with relative depth

For rod cases, Γ varies linearly in the main channel and floodplain from the peak value as shown in Figure 8. We proposal a first approximation of Γ as linear variation and the peak value is related to the drag force. The magnitude is significantly large and it could be transverse mixing due to drag force caused at the M/F interface rather than secondary flow.

A standard Γ of SKM is constant in a computing domain and Table 3 lists the averaged values of advection term in the main channel, side slope and floodplain domains.

Table 3 Experimental values of $\Gamma/\alpha\rho gHS_0$ for rod cases

	R1	R2	R3
MC	0.4253	0.4976	0.5416
ISW	0.6399	0.7541	0.6807
FP	0.4117	0.5297	0.5802

The predicted velocity and boundary shear stress for $\Gamma=0$, constant (standard) and linear approximation (new) are shown in Figures 9a ~9f. The prediction using the new Γ is much improved on the floodplain from the standard constant Γ in SKM model, but not in the main channel.

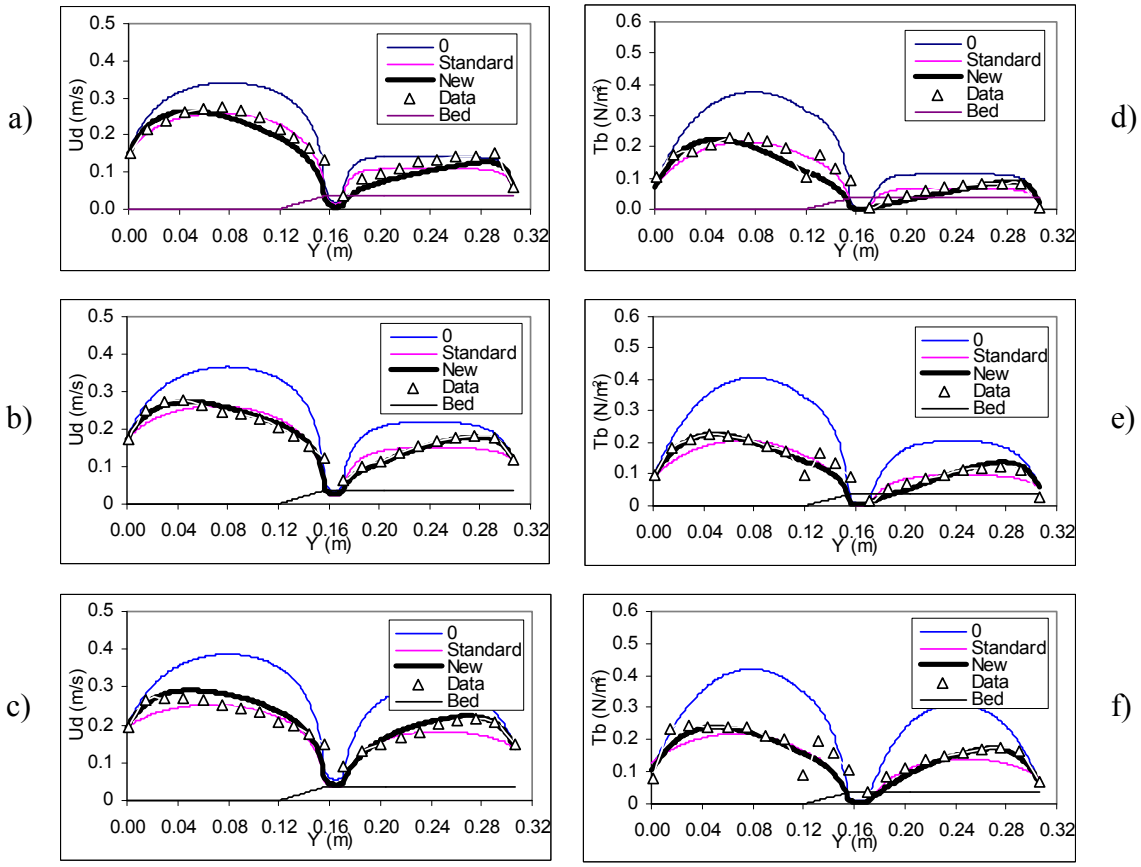

Figure 9 The predicted depth-averaged velocity (a~c) and boundary shear stress (d~f) at Dr=0.24, Dr=0.37 and Dr=0.52 respectively for rod case.

7. CONCLUSIONS

The measurements were conducted in compound channel along one-line rods at the edge of floodplain to investigate the effect of rods on flow structure, apparent shear force and boundary shear stress. In rod case, the apparent shear force at the main channel floodplain (M-F) interface significantly increases when compared with no rod case. A typical momentum transfer occurred at the M-F interface for compound channel is much less than no rod case, owing to drag force of rods. Drag force becomes predominant and larger than the main

channel wall and floodplain wall shear forces, and hence the location of the maximum velocity is shifted towards both walls in the main channel and floodplain. The boundary shear stress was significantly reduced due to drag force of rods in both main channel and floodplain. The first approximation of drag force with the relative water depth was obtained using the limited experimental data. The advection term was also defined by a first approximation in both main channel and floodplain for SKM. With using those approximations, SKM predicts a better distribution of depth averaged velocity and boundary shear stress in the cross section on floodplain in particular when compared to a standard constant advection term in SKM.

ACKNOWDGEMENTS

The work was funded by the Department of Civil and Building Engineering, Loughborough University. The first author wishes to acknowledge Loughborough University for sponsoring his PhD study.

REFERENCES

Igarashi, T. (1984), Characteristics of the flow around two circular cylinders, Bulletin of JSME, Vol. 27, No.233, pp. 2380-2387.

Knight D. W. and Lai C. J. (1985), Turbulent flow in compound channels and ducts, Proceedings of 2nd Int. Symp. On "Refined Flow Modelling and Turbulence Measurements", Iowa, USA, Hemisphere Publishing Co., pp. I21-1-I21-10.

Kouwen, N. and Fathi-Moghadam, M. (2000), Friction factors for coniferous trees along rivers, Journal of Hydraulic Engineering, 126(10), pp. 732–740.

Nepf H. M. and Vivoni E. R. (2000), Flow structure in depth-limited, vegetated flow, Journal of Geophysical Research, 105(c12), pp. 28, 547-28,557.

Nezu I. and Nakagawa H. (1993), Turbulence in Open-channel Flows, IAHR Monograph, A. A. Balkema, Rotterdam, Brookfield.

Nezu I. and Onitsuka K.(2001), Turbulent structures in partly vegetated open-channel flows with LDA and PIV measurements, Journal of Hydraulic Research, 39(6), pp. 629-642.

Pasche E. and Rouve´ G. (1985), Overbank flow with vegetatively roughened flood plains, Journal of Hydraulic Engineering, 111(9), pp. 1262–1278.

Petryk, S., and Bosmajian G., III. (1975), ''Analysis of flow through vegetation.'' J. Hydr. Div., ASCE, 101(7), pp. 871–884.

Rameshwaran P. and Shiono K. (2007), Quasi two-dimensional model for straight overbank flows through emergent vegetation on the floodplain, Journal of Hydraulic research, 45(3), 302-315.

Sellin R. H. J. (1964), A laboratory investigation into the interaction between the flow in the channel of a river and that over its flood plain, La Houille Blanche, (7), pp. 793-801.

Shiono K. and Knight D. W. (1989), Transverse and vertical Reynolds shear stress measurements in a shear layer region of a compound channel, Proc. 7th Int. Symp. On Turbulent Shear Flows, Stanford, U. S. A., pp. 28.1.1 – 28.1.6.

Shiono K. and Knight D. W. (1991), Turbulent open-channel flows with variable depth across the channel, Journal of Fluid Mech., 222, pp.617-646.

Sun X. (2007), Flow characteristics in compound channels with and without vegetation, PhD thesis, Loughborough University, UK.

Tominaga, A. and Nezu, I. (1991), Turbulent structure in compound open-channel flows, Journal of Hydraulic Engineering, 117(1), pp. 21 – 41.

Tsujimoto T. (1992), Spectral analysis of velocity and water surface fluctuationa appearing in an open channel with vegetated and non-vegetated regions in a cross-section, Proc. Of the 6th IAHR International Symposium on Stochastic hydraulics, Taipei, pp. 361-368.